

Research Article

Fatigue Stress Estimation of an Offshore Jacket Structure Based on Operational Modal Analysis

Bruna Nabuco ¹, **Marius Tarpø**,² **Ulf T. Tygesen**,³ and **Rune Brincker**¹

¹Technical University of Denmark, Department of Civil Engineering, Brovej 118, 2800 Kgs. Lyngby, Denmark

²Aarhus University, Department of Engineering, Inge Lehmanns Gade 10, 8000 Aarhus, Denmark

³Ramboll Oil and Gas, Department of Marine Structures, Bavnehøj 5, 6700 Esbjerg, Denmark

Correspondence should be addressed to Bruna Nabuco; brunabuco@gmail.com

Received 14 February 2020; Revised 22 April 2020; Accepted 6 May 2020; Published 30 May 2020

Academic Editor: Guanghui Zhao

Copyright © 2020 Bruna Nabuco et al. This is an open access article distributed under the Creative Commons Attribution License, which permits unrestricted use, distribution, and reproduction in any medium, provided the original work is properly cited.

Fatigue life assessment currently recommended by offshore standards is associated with a large number of uncertainties mainly related to the environmental loads and the numerical model. Recently, for economic reasons, the need for extending the lifetime of existing offshore structures led to the necessity of developing more accurate and realistic predicting models so that damage detection and maintenance can be optimized. This paper proposes the implementation of Structural Health Monitoring Systems in order to extract modal properties—such as mode shapes, natural frequencies, and damping ratios—throughout Operational Modal Analysis (OMA), which is the engineering field that studies the modal properties of systems under ambient vibrations or normal operating conditions. The identified modal properties of the structural system are the fundamental information to update a finite element model by means of an expansion technique. Then, the virtual sensing technique—modal expansion—is used to estimate the stress in the entire structure. Though existing models depend on the load estimation, the model based on OMA-assisted virtual sensing depends on the measured responses and assumes that the loads act as random vibrations. A case study using data from a real offshore structure is presented based on measurements recorded during normal operation conditions of an offshore tripod jacket. From strains estimated using OMA and virtual sensing, fatigue stresses are predicted and verified by applying the concept of equivalent stress range. Both estimated and measured strains are given as input data to evaluate the equivalent stress range and compared with each other. Based on this study, structural health monitoring estimates the fatigue stresses with high precision. As conclusion, this study describes how the fatigue can be assessed based on a more accurate value of stress and less uncertainties, which may allow extending the fatigue life of offshore platforms.

1. Introduction

Fatigue life is stated in terms of stress ranges that are produced by the variable loads imposed on a structure. The most common variable loads affecting offshore structures are the waves. Current existing models can predict the evolution of fatigue damage over time by estimating the loads based on wave statistics and applying them into a numerical model. Several approaches follow these models, as recommended by offshore design codes [1] and more recent studies, for instance, the fatigue methodology proposed by Mourão et al. [2] using local damage parameters. Because

uncertainties are associated with the environmental loads and to the numerical model, it yields to the use of safety factors underestimating the operational fatigue life of the offshore structure. These uncertainties could be reduced by monitoring the structure with the use of strain gauges. However, since fatigue sensitive joints are usually located in areas of difficult access and strain gauges are fragile and often unreliable for long time measurements, this approach is not appropriate for evaluating the strain histories of offshore structures in long-term periods. An alternative is proposed through the use of Operational Modal Analysis (OMA) [3] assisted virtual sensing [4]. This virtual sensing

approach estimates the strain response of a structure by continuously monitoring the structural responses with accelerometers, which are known as reliable for long time measurements. A modal decomposition is performed, and the experimental mode shapes are identified and expanded to all degrees of freedom (DOFs) of a finite element (FE) model. Thereby, a few sensors are used to estimate the strains of the entire structure only based on the structural responses and not on the loads, which are assumed to be random vibrations.

In the literature on OMA applied to offshore structures, most of the applications are related to offshore wind turbine structures. For instance, Dong et al. [5] researched on vibration response characteristics and OMA of one offshore wind power structure. Bajrić et al. [6] compared the damping ratio for offshore wind turbine structures by different modal identification techniques validated by real vibration measurements of an offshore wind turbine under nonoperating conditions. Ruzzo et al. [7] proposed the identification of the rigid body motions of a spar floating support for offshore wind turbines through OMA. The method applied to a numerical model based on a linear equation of motion has proven to be a viable method for output-only identification of floating structures.

In the literature on stress estimation, the modal expansion is one of the most popular process models, which is a linear transformation that expands the system response based on the identified mode shapes [8]. Hjelm et al. [9] presented a full-field strain estimation technique using the modal expansion and applied it to a laboratory structure and a lattice tower. By dividing the response of an offshore structure into two parts, Skafte et al. [10] expanded the low-frequency response using the quasi-static Ritz vectors and the high-frequency response using modal decomposition for estimating the strain responses on a scale model of an offshore platform using only the information from the accelerometers. Aiming to evaluate the strain estimation, Nabuco et al. [11] applied a reliability analysis on the estimated strain response of a scaled offshore platform and showed the relevance of strain estimation compared to the traditional design codes. Furthermore, the modal expansion has been applied to nonlinear systems. In this way, Nabuco et al. [12] used modal expansion based on parameters determined from a linear case and successfully estimated the strain responses of two scaled offshore platforms connected with a friction structure. Tarpø et al. [13] investigated the precision of estimating the strain response of a nonlinear system using the operational response of numerical simulations where local nonlinearities were introduced by adding friction to the test specimen. Also, Tarpø et al. [14] concluded that expanding experimental mode shapes can increase the accuracy of the stress estimation and introduced a quality measurement, *Normalised Error of Fatigue Damage*, for stress estimation based on the normalized fatigue damage, which takes amplitudes into account.

Strain estimation of an offshore jacket structure based on OMA focusing on fatigue assessment is the overall goal of this paper. By considering the operational loads as

random vibrations, the strain histories are predicted via the virtual sensing technique and then compared with strain gauge measurements. Moreover, the concept of equivalent stress range is introduced in order to verify the precision in terms of fatigue damage. Figure 1 presents a general scheme of the methodology adopted in this paper.

Monitoring data from a typical tripod jacket platform for oil and gas production in the Danish North Sea sector have been provided to validate the theory. Data from the same platform, Valdemar, have already been applied in previous studies. Dascotte et al. [15] presented a system for continuous stress monitoring of large structures using an updated finite element model and displacements measured at a limited number of GPS receiver locations. According to Skafte et al. [16], the measured displacements can be expanded with high precision and the expansion technique can be used for assessment of measurement uncertainties.

To the best of the authors' knowledge, the application of stress estimation on structures in operation is limited to offshore wind turbines [17–22], stadium [23], and lattice structure [9, 24, 25]. Thus, this paper adds important information to stress estimation by applying this technique on an operating offshore platform.

2. OMA Theory for Strain Estimation

Aiming to estimate the strains in any point of a structure using OMA, the first step is to measure the displacements in a few points of the structure using accelerometers. Then, a modal identification is undertaken to assess the dynamic properties of the structure, and on this basis, the mode shape vectors \mathbf{A} are estimated.

The estimated modal coordinates in function of time, $\hat{\mathbf{q}}(t)$, are identified through a relation between pseudoinverse of the mode shape matrix, \mathbf{A}^+ , and the measured displacements, $\mathbf{y}(t)$:

$$\hat{\mathbf{q}}(t) = \mathbf{A}^+ \mathbf{y}(t). \quad (1)$$

In the present study, the local correspondence (LC) principle [26] is used to relate experimental mode shapes to a subspace of mode shapes from an FE model. The linear relation is defined by the transformation matrix \mathbf{P} :

$$\mathbf{P} = \mathbf{B}_a \mathbf{A}, \quad (2)$$

where \mathbf{B}_a is the FE mode shape matrix containing only the DOFs of the experimental mode shape matrix.

The LC principle provides an optimal subspace of FE mode shapes for smoothing and expansion of the experimentally obtained mode shape matrix. Hence, the transformation matrix \mathbf{P} is used to obtain the expanded experimental mode shape matrix (full matrix), \mathbf{A}_{full} , composed of the total number of DOFs of the FE mode shape matrix, \mathbf{B} :

$$\mathbf{A}_{\text{full}} = \mathbf{B}\mathbf{P}. \quad (3)$$

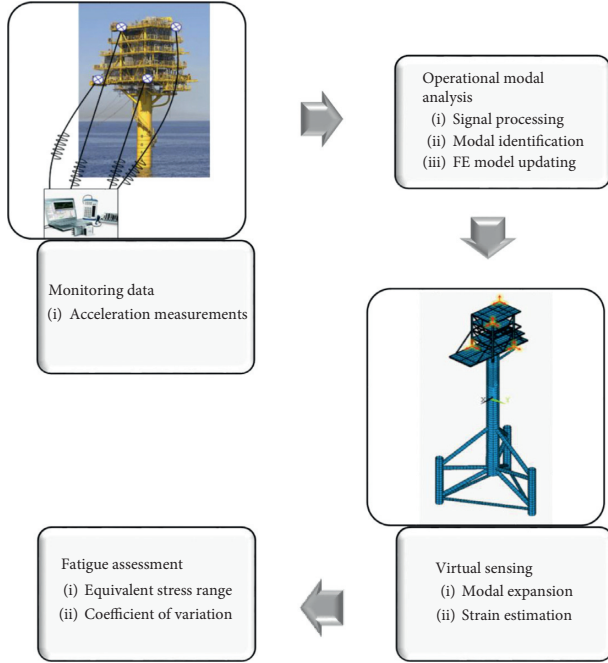


FIGURE 1: Methodology general scheme.

Because the modal coordinates for strains and displacements are the same, the strain history, $\hat{\boldsymbol{\varepsilon}}(t)$, is estimated as follows:

$$\hat{\boldsymbol{\varepsilon}}(t) = \mathbf{B}_\varepsilon \mathbf{P} \hat{\mathbf{q}}(t), \quad (4)$$

where \mathbf{B}_ε is the full strain mode shape matrix from the FE model. In this way, the strains at all DOFs of a structure are known with the use of OMA and virtual sensing only based on the measured displacements and not on the loads.

3. Fatigue Assessment

Currently, fatigue analyses for fatigue damage accumulation assessment of this type of structure are based on SN curves for welded structural components, hot-spot stress approach, and Palmgren-Miner law, according to design codes.

The fatigue damage considered here is modeled based on the SN fatigue approach under the assumption of linear cumulative damage, D , as per the Palmgren-Miner rule [27]. By dividing the stress cycles into j blocks, the accumulated fatigue damage is expressed as follows:

$$D = \sum_{i=1}^j \frac{n_i}{N_i} = \frac{1}{a} \sum_{i=1}^j n_i \cdot S_i^m, \quad (5)$$

where n_i is the number of stress cycles of the i^{th} block, N_i is the number of cycles to failure at a given constant stress range S_i , m is the SN curve slope parameter, and a is the SN curve intercept parameter.

From the fracture mechanics theory of fatigue, it is known that if the crack initiation phase is negligible, the slope of the SN curve, m , is identical to the exponent of the crack growth in Paris' law. This parameter depends mainly on the material

property, and most experimental data for structural steels, as in offshore structures, indicate that $m = 3$ [28].

The SN curve intercept parameter, a , depends on the geometry of the connection and type of weld. Since the methodology described in this paper is not focused on local fatigue assessment, the concept of equivalent stress range is introduced as a means to represent the spectral fatigue loading through only one equivalent stress range.

3.1. Equivalent Stress Range. According to [28], there is a constant amplitude stress range that causes the same fatigue damage as the sequence of variable amplitude stress ranges it replaces for the same number of cycles. This constant amplitude is known as the equivalent stress range.

This equivalence principle implies that the equivalent stress range, S_{eq} , is constant throughout the entire loading process and must give the same damage ratio as calculated using equation (5).

$$D = \frac{1}{a} N_t (S_{\text{eq}})^m, \quad (6)$$

where N_t is the total number of stress cycles, $N_t = \sum_i n_i$. By combining equations (5) and (6), the equivalent stress range can be expressed as follows:

$$S_{\text{eq}} = \left(\frac{1}{N_t} \sum_{i=1}^j n_i \cdot S_i^m \right)^{1/m}. \quad (7)$$

Note that the equivalent stress range established through equation (7) is independent of the SN curve intercept parameter.

4. Quality Assurance

The experimental modal properties, such as the natural frequencies and the mode shapes, are compared with the modal properties from the FE model. Comparing the natural frequencies is a straightforward procedure because in this case, we are dealing with single values. If the difference between two sets of values is less than a certain threshold value generally defined by self-experience and expected uncertainties or by prescribed values from standards, then we consider the result satisfactory. However, in order to compare mode shapes, a correlation measure is normally used because of many DOFs at each measured location.

The Modal Assurance Criterion (MAC) [29] is used to compare the experimental mode shape vectors, \mathbf{A} , with the FE mode shape matrix composed only of the same DOFs, \mathbf{B}_a , as shown in the following equation:

$$\text{MAC} = \frac{(\mathbf{A}^H \mathbf{B}_a)^2}{(\mathbf{A}^H \mathbf{A})(\mathbf{B}_a^H \mathbf{B}_a)}. \quad (8)$$

For checking the quality of the strain estimation, it is used as a quality assurance quantitative measurement in the time domain called Time Response Assurance Criterion (TRAC) [30]. Being $\hat{\boldsymbol{\varepsilon}}$ the estimated strains and $\boldsymbol{\varepsilon}$ the

measured strains, the TRAC values are estimated by means of the following equation:

$$\text{TRAC} = \frac{(\boldsymbol{\varepsilon}^T \hat{\boldsymbol{\varepsilon}})^2}{(\boldsymbol{\varepsilon}^T \boldsymbol{\varepsilon})(\hat{\boldsymbol{\varepsilon}}^T \hat{\boldsymbol{\varepsilon}})}. \quad (9)$$

Similar to the MAC, the TRAC is a tool used to determine the degree of correlation between two time traces. Values produced by both the MAC and TRAC will range from zero to one, where values approaching one indicate a good correlation. On the other hand, the TRAC might mislead the quality of strain estimation since it is independent of amplitude differences.

As the strain range is crucial on the fatigue damage estimation, Tarpø et al. [14] proposed a quality measurement based on the SN curve and the Palmgren-Miner rule called normalized error of fatigue damage (NEFD) described by the following equation:

$$\text{NEFD} = \frac{\sum_{i=1}^j \tilde{S}_i^m}{\sum_{i=1}^j S_i^m} - 1, \quad (10)$$

where NEFD equals to zero indicates a perfect estimation of strain, a negative value means an underestimation of fatigue damage, and a positive value indicates an overestimation of fatigue damage.

5. Case Study

A tripod jacket has been measured during normal operation in the North Sea in a water depth of 42.7 m (See Figure 2). The diameter of the main pile is 3.43 m with a thickness of 0.06 m at the mean water level (MWL). Data from accelerometers, strain gauges, and wave radars are provided defining 14 datasets. The duration of each dataset is one hour.

The advantage of the OMA-based stress estimation technique is to assess the responses of the structure in locations that are not easily accessible (e.g., in the vicinity of joints below the sea surface) using measurements obtained in easily accessible locations (e.g., along the topside). This is facilitated by four triaxial accelerometers positioned on the upper part of the structure corresponding to a total of 12 DOFs.

In addition, four strain gauges (SGs) are placed at the lowest feasible elevation: two at 11.5 m above MWL (Elevation 1) and two at 12.2 m above MWL (Elevation 2). At each elevation, one strain gauge is placed at 233 degree clockwise from North (Azimuth C) and the other at 143 degree (Azimuth D). Note that these strain gauges are intended to verify the stress estimation, but not for fatigue analysis since they are located far from the fatigue critical locations of the structure. Figure 3 illustrates the position of accelerometers and strain gauges.

The sea elevation has been measured at three locations, each one below a corner of the cellar deck. Based on the wave gauge measurements, Table 1 presents the values of significant wave height, H_S , and the peak period, T_P calculated for each data set.

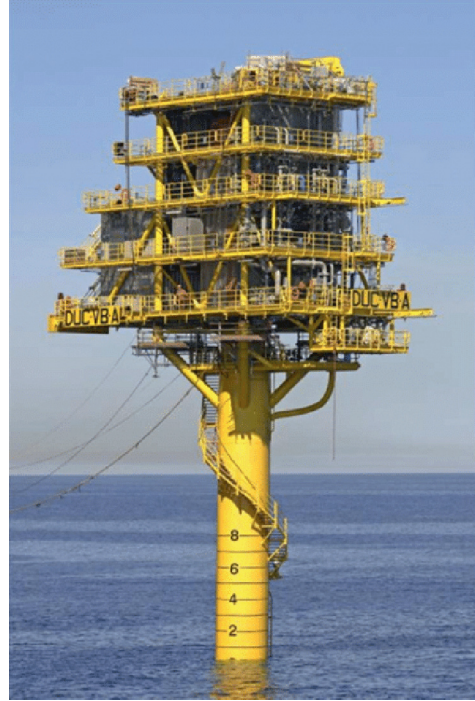


FIGURE 2: A photo of Valdemar tripod jacket [31].

It should be emphasized that only monitoring data from the accelerometers plays a role in the estimation of the strains. The strain gauge measurements are exclusively intended to verify the results. Also, the wave gauge data are solely for correlating the obtained results with the wave loads. Other environmental loads also contribute to the fatigue damage; however, only the wave measurements are available for this study.

5.1. Signal Processing. The response data are acquired by a sampling frequency of 128 Hz and later decimated by a factor of 20. Band-pass filtering using a Hanning tapering in the frequency domain is applied to both the acceleration and strain measurements. Tapering corresponding to the half size of the applied Hanning time window is applied in the beginning, from 0.4 Hz to 0.5 Hz, and at the end of the signal, from 1.5 Hz to 1.6 Hz. The low cut-off frequency is defined to simplify the model and remove the influence of the quasi-static response caused by waves. The high cut-off frequency is defined to limit the acquired data bandwidth to account only for the first three modes.

With the purpose of obtaining the displacements, the signal from accelerometers is then integrated twice using one-shot FFT-filtering with the shape of cosine tapering. A band-pass frequency-domain filter described by the two filter frequencies 0.5 Hz and 2.0 Hz is used only to suppress the signal close to DC and Nyquist.

5.2. Modal Identification. A modal identification is performed in the time domain to obtain the experimental modal properties, in particular, natural frequencies, damping ratios, and mode shapes. One of the simplest ways to perform

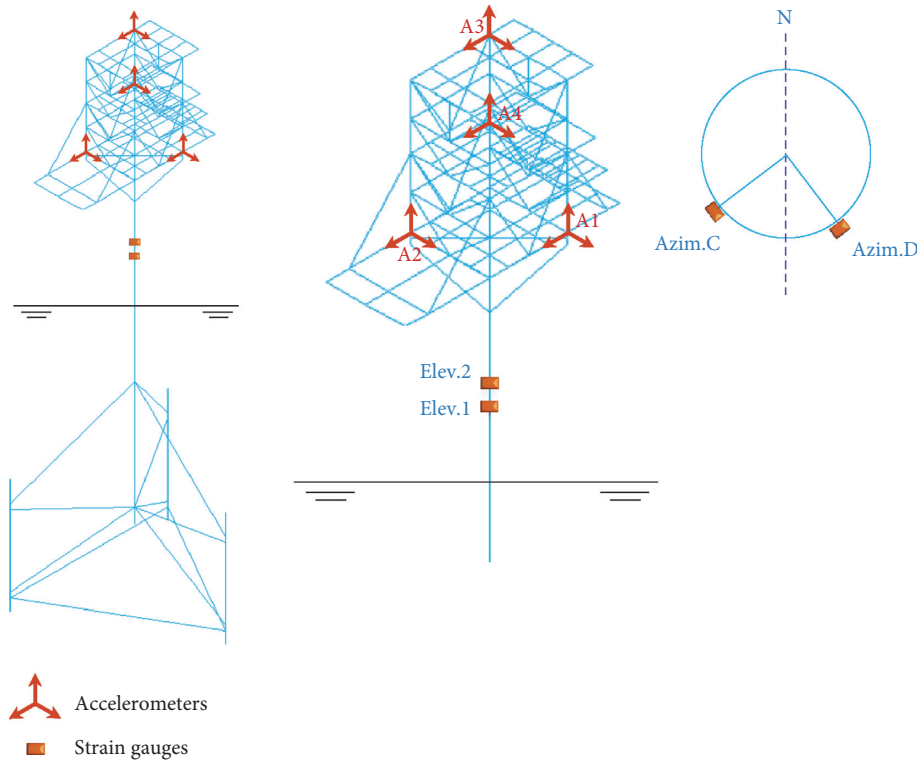


FIGURE 3: Position of sensors.

TABLE 1: Wave parameters.

| Dataset | H_s (m) | T_p (s) |
|---------|-----------|-----------|
| 1 | 1.12 | 6.49 |
| 2 | 1.16 | 7.52 |
| 3 | 1.17 | 6.28 |
| 4 | 1.29 | 5.20 |
| 5 | 1.45 | 5.97 |
| 6 | 1.67 | 6.33 |
| 7 | 1.68 | 5.87 |
| 8 | 2.26 | 6.46 |
| 9 | 2.51 | 6.77 |
| 10 | 4.57 | 11.11 |
| 11 | 4.71 | 12.05 |
| 12 | 4.78 | 11.18 |
| 13 | 4.97 | 12.37 |
| 14 | 5.15 | 11.79 |

OMA is to use autoregressive models on the free decays estimated as correlation functions [3]. The technique applied herein follows the same approach as the poly reference technique by Vold et al. [32], but using correlation functions instead of impulse response functions. By estimating the spectral density matrix as a function of frequency using the Welch averaging technique with a Hanning window and 50% overlap, the singular values of spectral density are obtained and plotted in Figure 4.

5.3. FE Modelling and Updating. Based on as-built technical drawings, an FE model of the offshore structure is created in ANSYS [33]. It consists of 1156 beam elements and 452 shell

elements. The topside has been simplified to include only the structural elements deemed most important for the first three structural modes. Only the primary structure has been modeled. The boundary conditions are assumed to be fixed at the bottom three supports in all DOFs.

As a conservative approach, the boundary conditions at the supports have been kept fixed and only the mass has been modified for calibrating the model. In case the soil stiffness was estimated, it could lead to an underestimation of the strains. Initially, the topside mass of 465 tons defined in the design of the platform has been considered through the material density of the beam elements in the topside. Later, the material density has been increased by 20% as a means to provide natural frequencies close to the measurements. Also, the topside mass had to be redistributed in an effort to improve the MAC value corresponded to the torsional mode. After performing this manual updating, the FE model dynamic properties are compared with the experimental dynamic properties from the modal identification results (see Table 2). Figure 5 illustrates the deformed shape of the FE model of the three identified modes.

5.4. Strain Responses. Using the FE model, modal expansion is performed through equations (2) and (3), and the strains are estimated at the location of each SG. Figure 6 shows the estimated and measured strains of dataset 14 obtained at Elevation 1 for both azimuths. Figure 7 displays the same comparison in the frequency domain from which it can be observed that the measured signal has a contribution from higher modes that are not accounted for in this study.

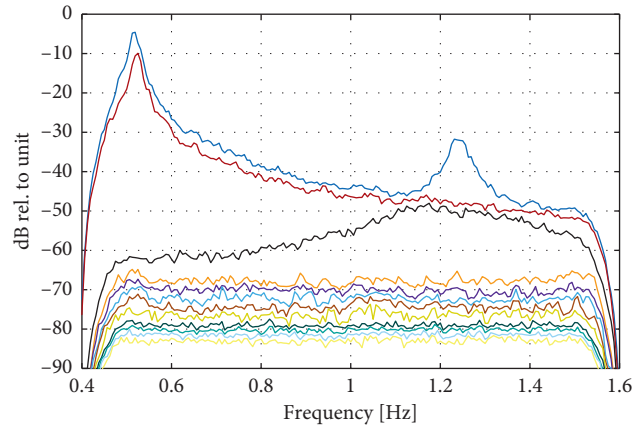


FIGURE 4: Singular values of spectral density.

TABLE 2: Comparison between experimental and numerical modal properties.

| | Mode 1 | Mode 2 | Mode 3 |
|---------------------------------|--------|--------|--------|
| Experimental frequency (Hz) | 0.514 | 0.527 | 1.234 |
| Numerical frequency (Hz) | 0.515 | 0.518 | 1.229 |
| Error (%) | -0.121 | 1.799 | 0.387 |
| Modal Assurance Criterion (MAC) | 0.998 | 0.997 | 0.982 |

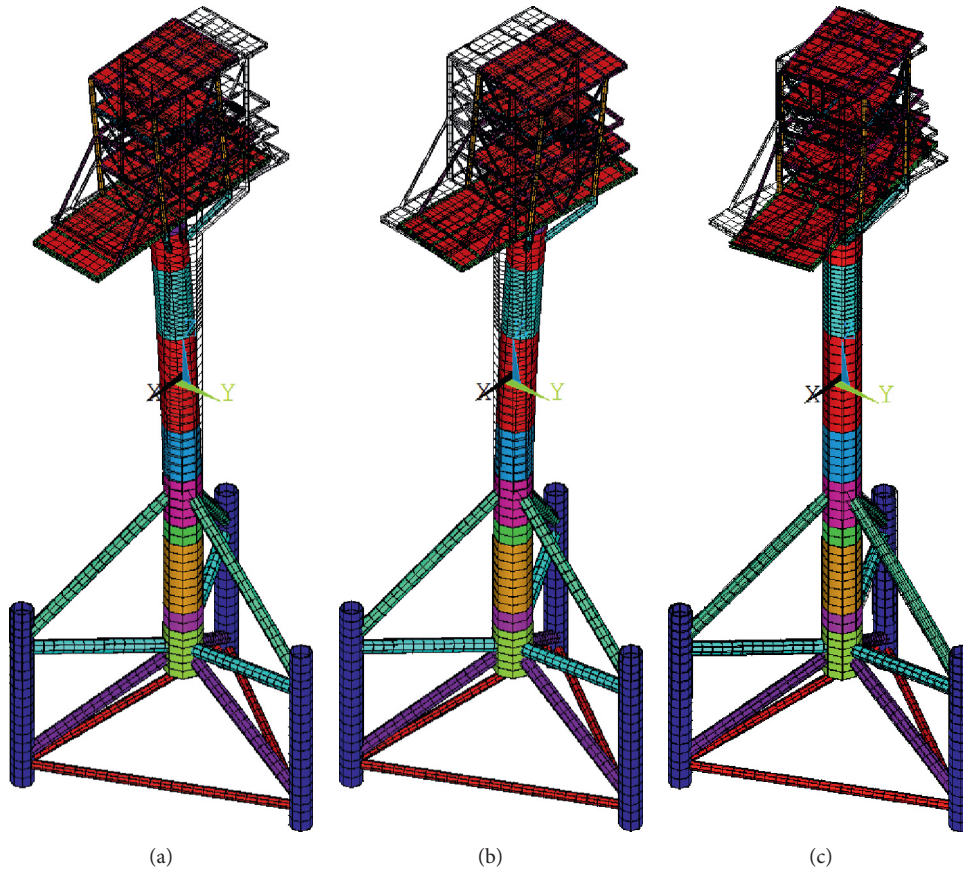


FIGURE 5: (a) First mode: bending moment in the longitudinal direction. (b) Second mode: bending moment in the transverse direction. (c) Third mode: torsion moment.

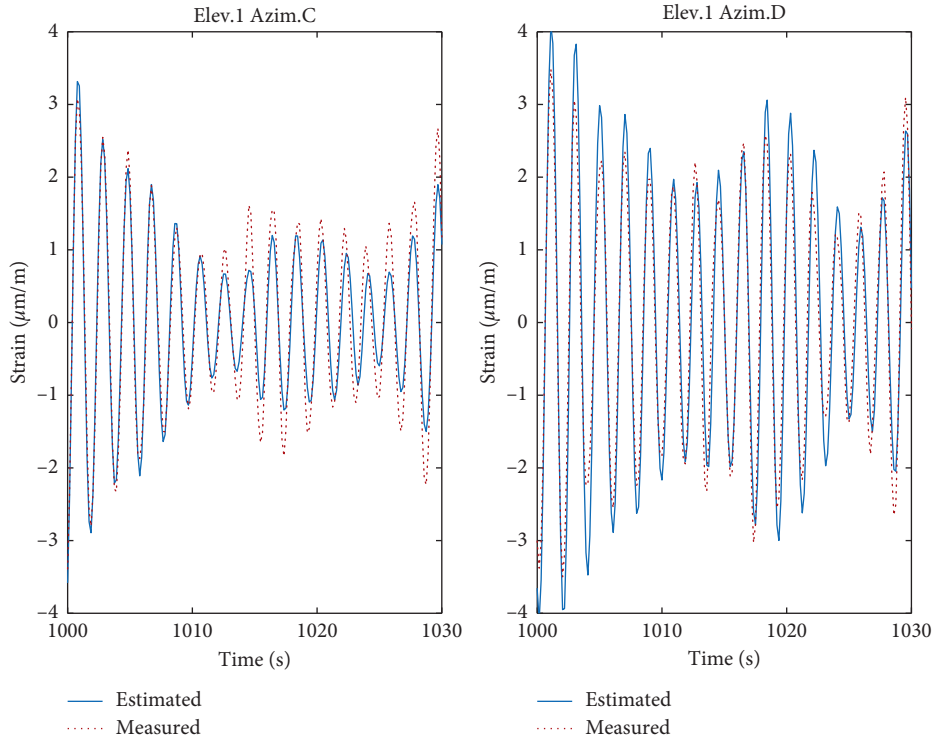


FIGURE 6: Strain history at Elevation 1 for dataset 14.

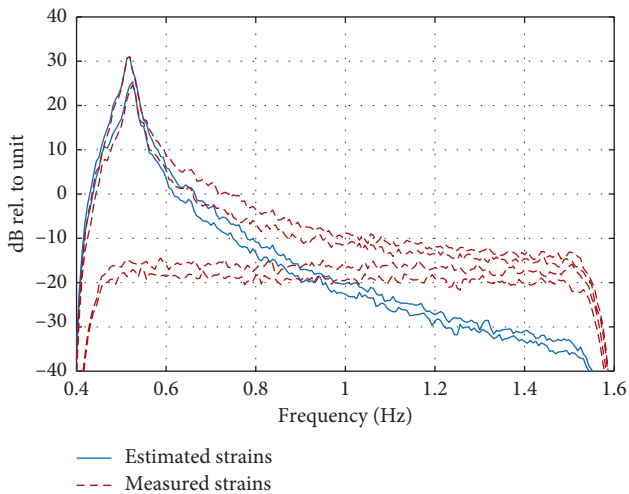


FIGURE 7: Spectrum plot of estimated and measured strains at Elevation 1 for dataset 14.

The accuracy of the strains $\hat{\epsilon}$, estimated via equation (4), is verified by comparison with the measured strains, ϵ , via TRAC values obtained using equation (9). Taking into account all 14 datasets, the TRAC values are between 92.5% and 94.5%, which indicates a high correlation between the experimental and numerical time signals.

The strain gauges are placed at the lowest feasible elevation, but still in a much higher elevation than the bottom support structure where the critical fatigue joints are usually located. For this reason, the strain values presented here are relatively small. However, throughout this study, the strains

have been successfully estimated and compared to strain gauge measurements, confirming that the FE model is reliable. Later, this FE model can be used to evaluate far-field stresses closer to the critical fatigue elements.

5.5. Verification of Tilt Influence. Offshore platforms are large structures that can easily have low natural frequencies, and one of the issues of using accelerometers at such low frequencies is the effect of the tilt of the structure introducing gravity effects on the acceleration measurements [3]. The influence of the tilt increases as the natural frequency of the structure decreases [3], becoming more relevant for frequencies lower than 0.1 Hz. Since the cut-off lower frequency for this case study is defined at 0.4 Hz, the very low frequencies are attenuated.

Considering the structure acting as a vertical clamped beam, a simplified calculation is made to quantify the influence of the tilt based on the structure height, h , the first mode natural angular frequency, ω_n , and the gravity acceleration, g . It is assumed that the deformation is due to its first mode of vibration only, and the acceleration of the structure is $\ddot{u} = \cos(\omega_n t)$.

By integrating twice the acceleration, the amplitude at the top is $u = \cos(\omega_n t)/\omega_n^2$. The tilting angle, θ , is approximately $\theta = 2u/h$. So, the absolute error in the measurement is $e = g\theta$. For the current case study, $h = 77$ m, $\omega_n = 3.14$ rad/s, and $g = 9.81$ m/s². In this case, the error relative to the acceleration is then $e/\ddot{u} = 2.6\%$. This means that what has been measured might correspond to a signal of approximately 2.6% larger than the actual response of the structure.

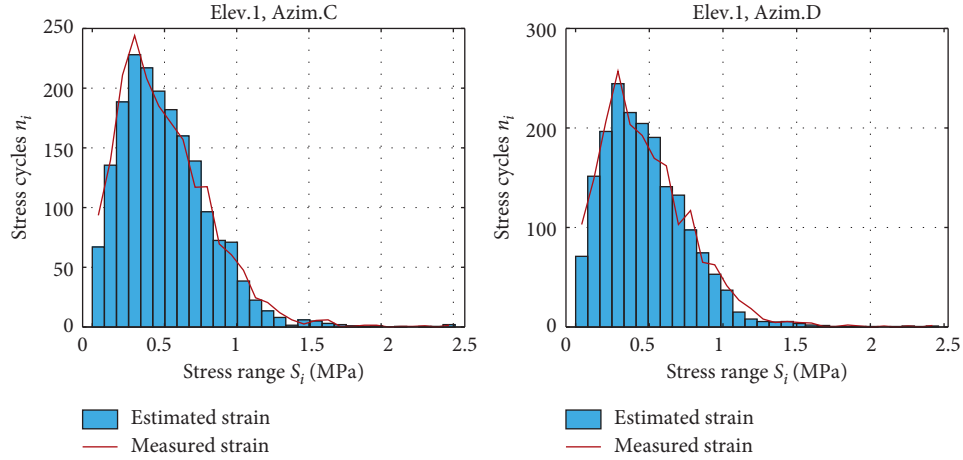


FIGURE 8: Stress histogram for dataset 14.

5.6. Fatigue Assessment. Stress histories are calculated from the strain responses and a Young modulus of 210 GPa. Afterward, the number of fatigue cycles of different stress ranges is assessed through the rainflow cycle counting algorithm [34, 35] for both the estimated and the measured stress histories. As a result, Figure 8 displays the stress histogram obtained for dataset 14 at Elevation 1.

The equivalent stress range is evaluated for all datasets using equation (7), from which the difference between the equivalent stress range calculated from the estimated strains and the one calculated from the measured strains has a standard deviation of 4.86% and a maximum value of 9.83%. Based on these results, Figure 9 presents the error of the equivalent stress range calculated from the estimated strains in relation to the one calculated from the measured strains. The x -axis exhibits the significant wave height associated with each dataset defined in Table 1.

It is worth mentioning that the application of the OMA-based virtual sensing technique aims to reduce the uncertainties in the stress values, and this can be evaluated in terms of fatigue damage through the concept of equivalent stress range. Therefore, the use of this technique would lead to the same number of uncertainties on the stress range either performing a stochastic fatigue analysis or a simplified fatigue analysis.

Regarding fatigue damage accuracy, the error between responses from estimated and measured strains is evaluated by means of equation (10). The NEFD results in function of the significant wave height are plotted in Figure 10 for all 14 datasets, and a linear trend line is added for each strain gauge position.

5.7. Coefficient of Variation. In inspection planning, the uncertainty on the stress history is included in a coefficient of variation (CoV). For offshore jacket structures, the CoV is typically ranging from 0.10 to 0.15 [36].

Based on the estimated stress results, Figure 11 presents the CoV calculated for each dataset. By adding the estimated stress history of all datasets, a time history of 14 hours is available. The CoV for this longer time history is equal to 0.0417, 0.0276, 0.0458, and 0.0376, at the locations Elev.1 Azim.C, Elev.1 Azim.D, Elev.2 Azim.C, and Elev.2 Azim.D,

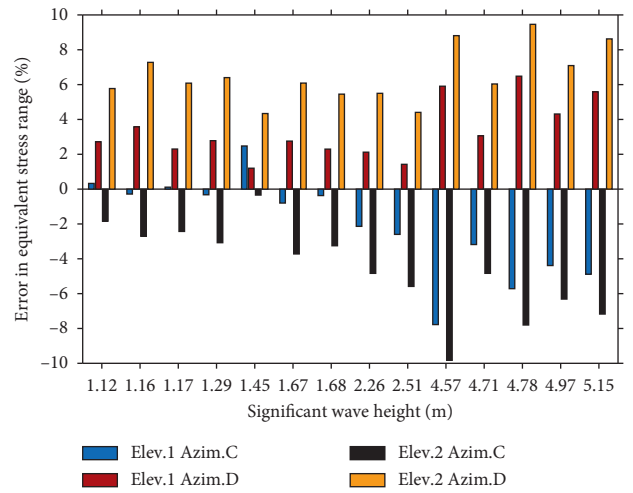


FIGURE 9: Error in equivalent stress range based on initial azimuth values.

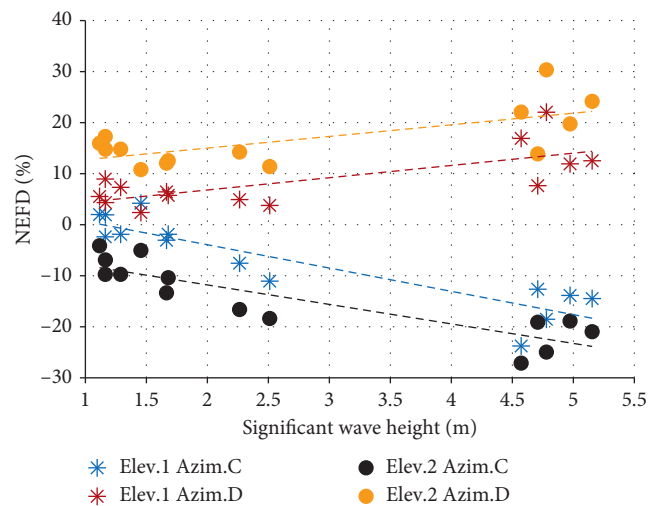


FIGURE 10: Normalized error of fatigue damage (NEFD) based on initial azimuth values.

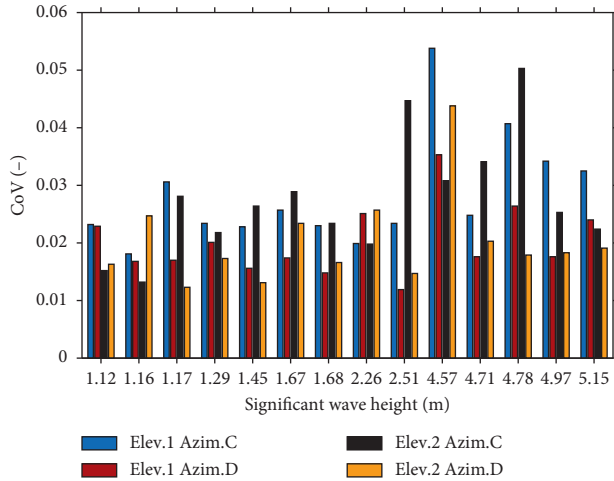


FIGURE 11: Coefficient of variation (CoV).

respectively. In addition, the bias is found to be 1.0474, 0.985, 1.0763, and 0.9572, respectively.

5.8. Sensitivity Analysis. It is observed that the equivalent stress range estimation is sensitive to the angular position of the SG defined by the azimuth value. Small variations of azimuth can lead to considerable changes in the stress range estimation. Such behavior is not significant concerning the elevation position of the SG.

For this reason, a sensitivity analysis of the SG azimuth is conducted. Table 3 presents the azimuth angle that reduces most of the error between estimated and measured fatigue damage as well as the absolute mean and the maximum values of NEFD considering the optimal azimuth angle. Moreover, it has been observed that the NEFD values vary between 6% and 9% per azimuth degree depending on the SG position. Note that, for this case study, each degree corresponds to 3 cm.

By applying the optimal azimuth angles, the error between the equivalent stress range calculated from the estimated strains and the one from the measured strains is reassessed and shown in Figure 12. The results of NEFD are also revised as illustrated in Figure 13. It can be noticed that the accuracy of the fatigue damage at Azimuth *D* is higher compared with Azimuth *C*. Further investigation must be carried out, for instance, to evaluate the influence of the main wave direction on the stress estimation results.

5.9. Results and Discussions. Quality measurements have been applied to the stress estimation findings to quantify the correlation between estimated and measured responses. The TRAC values are between 92.5% and 94.5%, which is considered to be high especially for the case of measurements from a real offshore structure and confirms that the strains of a structure can be estimated with good precision by performing structural health monitoring.

A standard deviation of 4.86% and a maximum difference of 9.83% have been found when comparing the equivalent stress ranges based on the estimated strains with the ones based on the measurements. By using a simplified

TABLE 3: Optimal azimuth of SG position.

| SG position (-) | Initial azimuth (deg) | Optimal azimuth (deg) | NEFD | |
|-----------------|-----------------------|-----------------------|----------------|---------|
| | | | Abs. mean. (%) | Max (%) |
| Elev.1 Azim.C | 233.0 | 231.5 | 8.30 | -15.62 |
| Elev.1 Azim.D | 143.0 | 144.5 | 4.76 | 9.64 |
| Elev.2 Azim.C | 233.0 | 230.5 | 7.31 | -13.95 |
| Elev.2 Azim.D | 143.0 | 145.5 | 4.69 | 8.67 |

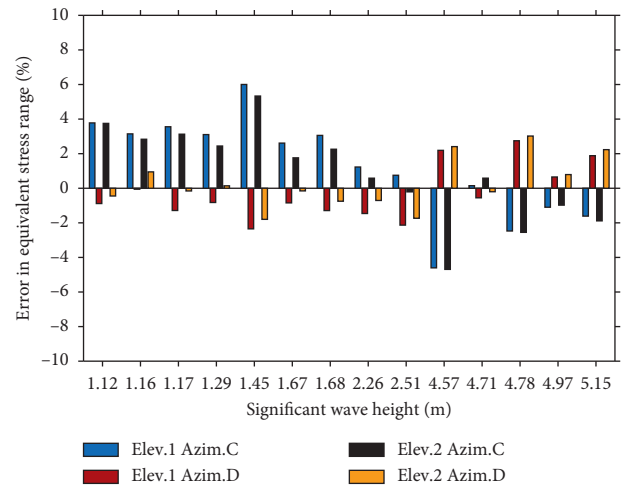


FIGURE 12: Error in equivalent stress range based on optimal azimuth values.

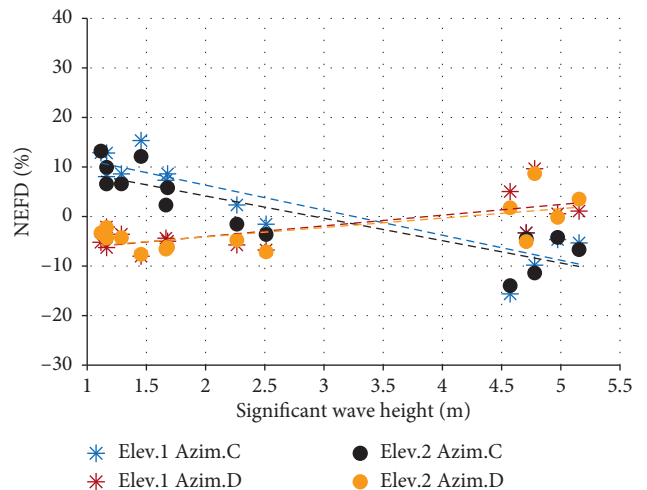


FIGURE 13: Normalized error of fatigue damage (NEFD) based on optimal azimuth values.

method, it was noticed that the influence of the tilt can increase the accuracy of the estimated stresses by 2.6%.

NEFD indicates a small difference in the fatigue damage estimation when the structure is excited by small waves, but

the error increases as the wave height increases, exceeding 20% when H_s is around $5m$. The fatigue damage is dependent on the stress range by the exponent m as can be seen in equation (6). Consequently, it is expected that the error in the fatigue damage, characterized by NEFD, is higher than the error in the equivalent stress range.

From the results, the CoV on the stress history is lowered to below 0.05. According to this outcome, the number of on-site inspections can be reduced significantly since it directly depends on the uncertainty on the stress history.

In addition, a sensitivity analysis was conducted concerning the strain gauge location. Based on the available strain gauge measurements of the case study, it was found that the influence of the selected azimuth can vary the normalized error up to 9% per each azimuth degree, which means that small changes in the azimuth of the strain gauge position can significantly reduce the error in the fatigue damage estimation.

6. Conclusions and Future Work

A methodology based on monitoring data is proposed as an alternative to replacing the design fatigue model of offshore structures with a more accurate model. On this basis, structural responses of a real tripod jacket platform have been estimated through OMA-assisted virtual sensing. The equivalent stress range has been determined from OMA-based strain histories from which it could be observed that the reduced uncertainties effectively impacted on the assessment of the accumulated fatigue damage. The results are sensitive to the strain gauge angular position around the structure cross section. The accuracy is even higher when considering the influence of the tilt. Among other advantages, the lowered CoV on the stress history yields a reduction in the number of inspections on the offshore structure.

Progress has been made in the estimation of fatigue stresses based on monitoring data. However, some investigations might be addressed in future studies, for instance, the effect of the quasi-static response caused by waves in the estimated responses. Also, more information could be assessed if measurements of other environmental loads were made available for comparison with the results. Furthermore, placing a strain gauge closer to the support of a structure, even for a short term period, could provide data that would result in more critical accumulated damage values.

Subsequently, a reliability analysis will be assessed based on the results of this study to evaluate the potential of a fatigue life extension followed by a value of information analysis to quantify the economic gain of the proposed approach.

Notations

| | |
|-----------------|---|
| $\hat{\cdot}$: | Estimated value |
| $.^T$: | Transpose operator |
| $.^H$: | Hermitian operator |
| A : | Experimental mode shape matrix |
| A_{full} : | Expanded experimental mode shape matrix |

| | |
|--------------------|--|
| B : | Finite element mode shape matrix |
| B_a : | Finite element mode shape matrix |
| B_ε : | Full strain mode shape matrix |
| P : | Transformation matrix |
| S : | Stress range vector |
| $q(t)$: | Modal coordinate vector |
| $y(t)$: | Displacement vector |
| $\varepsilon(t)$: | Strain vector |
| a : | SN curve intercept parameter |
| D : | Accumulated fatigue damage |
| e : | Error |
| g : | Gravity acceleration |
| h : | Structure height |
| i, j : | Indices |
| m : | Crack growth parameter |
| n_i : | Number of stress cycles in block i |
| N_i : | Number of stress cycles until failure in block i |
| N_t : | Total number of stress cycles until failure |
| S_{eq} : | Equivalent stress range |
| u : | Amplitude at the top of the structure |
| θ : | Tilting angle |
| ω_n : | Natural angular frequency |
| MAC: | Modal Assurance Criterion |
| TRAC: | Time Response Assurance Criterion |
| NEFD: | Normalized error of fatigue damage. |

Data Availability

The measured data used to support the findings of this study were supplied by the Danish Hydrocarbon Research and Technology Centre (DHRTC) under license. All the information about the data presented in this article is accepted for publication by DHRTC. Further information about the data cannot be made freely available.

Conflicts of Interest

The authors declare that there are no conflicts of interest regarding the publication of this paper.

Acknowledgments

The authors gratefully acknowledge the funding received from the Centre for Oil and Gas–DTU/Danish Hydrocarbon Research and Technology Centre (DHRTC).

References

- [1] DNVGL, “Fatigue design of offshore steel structures,” DNV GL AS, Høvik, Norway, 2016.
- [2] A. Mourão, J. A. F. O. Correia, B. V. Vila et al., “A fatigue damage evaluation using local damage parameters for an offshore structure,” *Proceedings of the Institution of Civil Engineers-Maritime Engineering*, 2020.
- [3] R. Brincker and C. E. Ventura, *Introduction to Operational Modal Analysis*, John Wiley & Sons, Hoboken, NJ, USA, 2015.
- [4] L. Liu, S. M. Kuo, and M. Zhou, “Virtual sensing techniques and their applications,” in *Proceedings of the 2009 International Conference On Networking, Sensing And Control*, IEEE, Okayama, Japan, pp. 31–36, March 2009.

- [5] X. Dong, J. Lian, H. Wang, T. Yu, and Y. Zhao, "Structural vibration monitoring and operational modal analysis of offshore wind turbine structure," *Ocean Engineering*, vol. 150, no. 92, pp. 280–297, 2018.
- [6] A. Bajrić, J. Høgsberg, and F. Rüdinger, "Evaluation of damping estimates by automated operational modal analysis for offshore wind turbine tower vibrations," *Renewable Energy*, vol. 116, pp. 153–163, 2018.
- [7] C. Ruzzo, G. Failla, M. Collu, V. Nava, V. Fiamma, and F. Arena, "Operational modal analysis of a spar-type floating platform using frequency domain decomposition method," *Energies*, vol. 9, no. 11, 2016.
- [8] D. C. Kammer, "Test-analysis model development using an exact modal reduction," *The International Journal of Analytical and Experimental Modal Analysis*, Society for Experimental Mechanics, Bethel, CT, USA, 1987.
- [9] H. Hjelm, J. D. Sørensen, R. Brincker, K. Munch, and J. Graugaard-Jensen, "Reduction in inspection costs for dynamic sensitive steel structures by modal based fatigue monitoring," in *Proceedings of the ASME 2005 International Conference on Ocean, Offshore and Arctic Engineering*, ASMC, Fort Lauderdale, FL, USA, pp. 245–252, June 2008.
- [10] A. Skafte, J. Kristoffersen, J. Vestermark, U. T. Tygesen, and R. Brincker, "Experimental study of strain prediction on wave induced structures using modal decomposition and quasi static Ritz vectors," *Engineering Structures*, vol. 136, pp. 261–276, 2017.
- [11] B. Nabuco, H. Brüske, M. H. Faber, and R. Brincker, "A first step in quantifying the value of OMA based fatigue stress monitoring," in *Proceedings of the 8th International Operational Modal Analysis Conference*, ASMC, Copenhagen, Denmark, May 2019.
- [12] B. Nabuco, M. Tarpø, A. Aissani, and R. Brincker, "Reliability analysis of offshore structures using OMA based fatigue stresses," in *Proceedings of the ASME 2017 36th International Conference on Ocean, Offshore and Arctic Engineering*, ASMC, Trondheim, Norway, June 2017.
- [13] M. Tarpø, T. Friis, B. Nabuco, S. Amador, E. Katsanos, and R. Brincker, "Operational modal analysis based stress estimation in friction systems," in *Proceedings of the Society for Experimental Mechanics Series*, vol. 1, SEM, Reno, NV, USA, pp. 143–153, June 2019.
- [14] M. Tarpø, B. Nabuco, C. Georgakis, and R. Brincker, "Expansion of experimental mode shape from operational modal analysis and virtual sensing for fatigue analysis using the modal expansion method," *International Journal of Fatigue*, vol. 130, Article ID 105280, 2020.
- [15] E. Dascotte, J. Strobbe, and U. T. Tygesen, "Continuous stress monitoring of large structures," in *Proceedings of the 5th International Operational Modal Analysis Conference-IOMAC'13*, IOMAC, Guimaraes, Portugal, pp. 1–10, May 2013.
- [16] A. Skafte, U. T. Tygesen, and R. Brincker, "Expansion of mode shapes and responses on the offshore platform valdemar," *Dynamics of Civil Structures*, vol. 4, pp. 35–41, 2014.
- [17] N. Noppe, K. Tatsis, E. Chatzi, C. Devriendt, and W. Weijtjens, "Fatigue stress estimation of offshore wind turbine using a kalman filter in combination with accelerometers," in *Proceedings of the ISMA 2018*, p. 9, ISMA, Heverlee, Belgium, November 2018.
- [18] K. Maes, A. Iliopoulos, W. Weijtjens, C. Devriendt, and G. Lombaert, "Dynamic strain estimation for fatigue assessment of an offshore monopile wind turbine using filtering and modal expansion algorithms," *Mechanical Systems and Signal Processing*, vol. 76–77, pp. 592–611, 2016.
- [19] K. Maes, G. De Roeck, G. Lombaert et al., "Continuous strain prediction for fatigue assessment of an offshore wind turbine using kalman filtering techniques," in *Proceedings of the 2015 IEEE Workshop on Environmental, Energy, and Structural Monitoring Systems (EESMS)*, IEEE, Trento, Italy, pp. 44–49, July 2015.
- [20] M. Henkel, W. Weijtjens, and C. Devriendt, "Validation of virtual sensing on subsoil strain data of an offshore wind turbine," in *Proceedings of the 8th International Operational Modal Analysis Conference-IOMAC*, vol. 19, p. 10, IOMAC, Copenhagen, Denmark, May 2019.
- [21] A. Iliopoulos, W. Weijtjens, D. Van Hemelrijck, and C. Devriendt, "Fatigue assessment of offshore wind turbines on monopile foundations using multi-band modal expansion," *Wind Energy*, vol. 20, no. 8, pp. 1463–1479, 2017.
- [22] A. Iliopoulos, W. Weijtjens, D. Van Hemelrijck, and C. Devriendt, "Full-field strain prediction applied to an offshore wind turbine," in *Model Validation and Uncertainty Quantification*, S. Atamturktur, T. Schoenherr, B. Moaveni, and C. Papadimitriou, Eds., vol. 3, pp. 349–357, Springer International Publishing, Berlin, Germany, 2016.
- [23] W. Lu, J. Teng, Q. Zhou, and Q. Peng, "Stress prediction for distributed structural health monitoring using existing measurements and pattern recognition," *Sensors*, vol. 18, no. 2, p. 419, 2018.
- [24] J. Graugaard-Jensen, R. Brincker, H. P. Hjelm, and K. Munch, "Modal based fatigue monitoring of steel structures," in *Proceedings of 6th International Conference on Structural Dynamics*, pp. 305–310, Paris, France, September 2005.
- [25] H. P. Hjelm, R. Brincker, J. Gaugaard-Jensen, and K. Munch, "Determination of stress histories in structures by natural input modal analysis," in *Proceedings of the IMAC XXIII International Modal Analysis Conference*, vol. 12, Society for Experimental Mechanics, Orlando, FL, USA, pp. 838–844, February 2005.
- [26] R. Brincker, A. Skafte, M. López-Aenlle, A. Sestieri, W. D'Ambrogio, and A. Canteli, "A local correspondence principle for mode shapes in structural dynamics," *Mechanical Systems and Signal Processing*, vol. 45, no. 1, pp. 91–104, 2014.
- [27] A. Palmgren, "Die lebensdauer von kugellagern," *VDI-zeitschrift*, vol. 64, pp. 339–341, 1924.
- [28] A. Almarnaess, *Fatigue Handbook: Offshore Steel Structures*, Tapir Publishers, Flatasen, Norway, 1985.
- [29] R. Allemang, "The modal assurance criterion—twenty years of use and abuse," *Sound and Vibration*, vol. 37, no. 8, 2003.
- [30] P. Avitabile and P. Pingle, "Prediction of full field dynamic strain from limited sets of measured data," *Shock and Vibration*, vol. 19, no. 5, pp. 765–785, 2012.
- [31] A. Wicks, "Structural health monitoring," in *Proceedings of the 32nd IMAC, A Conference and Exposition on Structural Dynamics, 2014*, vol. 5, Society for Experimental Mechanics Series, Orlando, FL, USA, 2014.
- [32] H. Vold, J. Kundrat, G. T. Rocklin, and R. Russell, "A multi-input modal estimation algorithm for mini-computers," in *Proceedings of the SAE International Congress and Exposition*, Detroit, MI, USA, February 1982.
- [33] ANSYS, *ANSYS Mechanical APDL*, ANSYS, Canonsburg, PA, USA, 2011.
- [34] ASTM, "Standard practices for cycle counting in fatigue analysis," Technical Report, ASTM International, West Conshohocken, PA, USA, 2005.

- [35] A. Niesony, "Determination of fragments of multiaxial service loading strongly influencing the fatigue of machine components," *Mechanical Systems and Signal Processing*, vol. 23, no. 8, pp. 2712–2721, 2009.
- [36] M. H. Faber, D. Straub, J. D. Sørensen, and J. Tychsen, "Field implementation of RBI for jacket structures," *Safety and Reliability*, vol. 2, pp. 295–303, 2003.